The International Archives of the Photogrammetry, Remote Sensing and Spatial Information Sciences, Volume XLIX-B3-2026
XXV ISPRS Congress 2026 “From Imagery to Understanding”, Commission III, 4–11 July 2026, Toronto, Canada

POD-AM-HAR: Cycle-to-Cycle Forecasting of Land Surface Dynamics in Latent Space*

Weidong Tang[1], Zheng Zhang[2]

[1] School of Electronic Engineering, Beijing University of Posts and Telecommunications,Beijing, China -twd206@bupt.edu.cn
[2] Aerospace Information Research Institute, CAS, Beijing, China - zhangzheng@aircas.ac.cn

Keywords: NDVI Time Series Forecasting, Latent Space Dynamics,Cycle-to-Cycle Prediction, Harmonic Analysis, Proper Orthogonal Decomposition (POD), Land Surface Evolution.

Abstract

Land surface dynamics exhibit strong periodic patterns, yet their interannual variations pose challenges for accurate forecasting. This paper proposes a POD-AM-HAR framework that shifts prediction from point-wise to cycle-to-cycle forecasting. The framework integrates Proper Orthogonal Decomposition for dimensionality reduction, Harmonic analysis Ridge regularization for small-sample stability. Validation on 10-year MODIS NDVI data from Ningxia, China, shows the framework effectively captures interannual evolution and maintains robust performance with limited training cycles.

1. Introduction

Satellite observations have accumulated extensive time-series imagery, capturing land surface changes with unprecedented temporal coverage. A critical challenge lies in how to accurately forecast future land surface states—a task essential for applications ranging from agricultural monitoring to disaster preparedness. Can a data-driven approach provide a viable solution for such forecasting tasks?

In recent years, research on complex systems has revealed that many seemingly highly complex high-dimensional systems often possess lower-dimensional dominant dynamical structures. That is, system evolution can be described more compactly and stably in an appropriate low-dimensional representation space (Gao, 2024). Given this insight, rather than performing forecasting directly in the original high-dimensional observation space—an approach plagued by the curse of dimensionality—an alternative is to conduct prediction in a latent space. A well-constructed latent space can substantially reduce spatial dimensionality while preserving the essential information needed to reconstruct the original high-dimensional space with minimal error. Such a reduction enables efficient learning of temporal dynamics and facilitates robust long-term forecasting.

In constructing the latent space, we first consider the case where it is a linear subspace (LS), as such a subspace can be efficiently constructed via singular value decomposition (SVD) of solution snapshot matrices. This linear approach provides a tractable foundation for forecasting, as it separates spatial structures from temporal coefficients.

Based on this principle, the three key steps that constitute the foundations of latent-space forecasting are: (i) data compression from the high-dimensional observation space to a lower-dimensional latent representation; (ii) learning the temporal evolution dynamics within this lower-dimensional space; and (iii) reconstructing future high-dimensional states from the predicted latent trajectories.

This paper introduces the POD-AM-HAR framework for forecasting land surface evolution via latent space dynamics. The framework shifts the prediction mode from point-wise to cycle-to-cycle forecasting by exploiting the strong periodicity of land surface processes, where $\mathbf{u}(x, y, t_i + T) \approx \mathbf{u}(x, y, t_i)$. Proper Orthogonal Decomposition (POD) first reduces high-dimensional observations into orthogonal spatial modes and corresponding temporal coefficients, capturing the dominant variability patterns. Then, Amplitude-Modulated Harmonic Analysis with Ridge regularization (AM-HAR) models these coefficients as a sum of harmonic components with cycle-varying amplitudes, overcoming the limitation of fixed waveforms in conventional harmonic analysis. By integrating these two approaches, the POD-AM-HAR framework establishes a regression-based forecasting methodology in a low-dimensional subspace, achieving both computational efficiency and predictive accuracy.

To validate the method, ten years of NDVI data from the Ningxia region was applied demonstrating its feasibility for modeling land surface processes.

2. Study Area, Data and Methods Overview

2.1 Study Area and Data

This paper selects the entire Ningxia Hui Autonomous Region as the study area, owing to its pronounced spatial heterogeneity in topography, hydrology, and climate. Located in the middle-upper reaches of the Yellow River in northwest China (35°01′–39°23′ N, 104°17′–107°39′ E), Ningxia encompasses three dominant geomorphological types: the Loess Plateau in the south, the Ordos Platform in the northeast, and alluvial floodplains along the Yellow River. The terrain generally slopes from southwest to northeast, with elevations ranging from 1,100 to 1,200 m. Prominent mountain ranges—including Liupan Shan, Luo Shan, and Helan Shan—create diverse microclimates across the region.

The experimental data used in this study are derived from the MOD13A2 product—the MODIS/Terra Vegetation Indices 16-Day L3 Global 1 km SIN Grid product—spanning the period from 2010 to 2020. The

* This research was funded by the Science and Disruptive Technology Program, AIRCAS (No.E3Z211010F)

dataset was downloaded from the NASA LAADS website (https://ladsweb.modaps.eosdis.nasa.gov/missions-and-measurements/products/MOD13A2). This product provides vegetation indices with a temporal resolution of 16 days and a spatial resolution of 1 km.

2.2 Method Overview

2.2.1 POD-AM-HAR Framework In Figure 1, we present a conceptual workflow of the proposed POD-AM-HAR framework for learning the latent space dynamics of land surface evolution from image sequences. The framework consists of three modular stages. First, we apply Proper Orthogonal Decomposition (POD) to the input image sequence, projecting the high-dimensional observations onto a low-dimensional subspace. This yields a set of spatial basis functions $\mathbf{\Phi}_k(x)$ (POD modes) that capture the dominant coherent structures, along with their associated temporal coefficients $\mathbf{a}_k(t)$that encode the time-varying behavior of the system.Since remote sensing data exhibit strong periodicity, $\mathbf{a}_k(t)$ also shows strong periodicity, and its period is assumed to be T, we then reconstruct a continuous-time dynamical model for these temporal coefficients $\mathbf{a}_k(t)$ using cycle-to-cycle Amplitude-Modulated Harmonic Analysis with Ridge regularization, that is, let $\mathbf{c}_j \in \mathbb{R}^T$ denote the j-th cycle of the original data $\mathbf{a}_k(t)$, and $\mathbf{c}_j = [\mathbf{a}_{(j-1)T+1}, \mathbf{a}_{(j-1)T+2}, \cdots, \mathbf{a}_{jT}]'$. We learn a dynamic model:

$$\mathbf{c}_{j+1} = \mathcal{F}(\mathbf{c}_j) + \boldsymbol{\varepsilon}_j \tag{1}$$

by a AM-HAR model as

$$c_j(t) = a_{0,j} + \sum_{k=1}^{K} \left[a_{k,j} \cos\left(\frac{2\pi kt}{T}\right) + b_{k,j} \sin\left(\frac{2\pi kt}{T}\right) \right] + \varepsilon_j(t) \tag{2}$$

Finally, the predicted temporal coefficients are projected back to the original high-dimensional space via the precomputed POD basis, generating future snapshots of land surface evolution. This POD-AM-HAR pipeline offers an interpretable, physics-informed approach that explicitly separates spatial structure extraction from temporal dynamics modeling, making it particularly suitable for analyzing quasi-periodic land surface phenomena such as vegetation phenology, seasonal water body variations, and cyclic land use patterns.

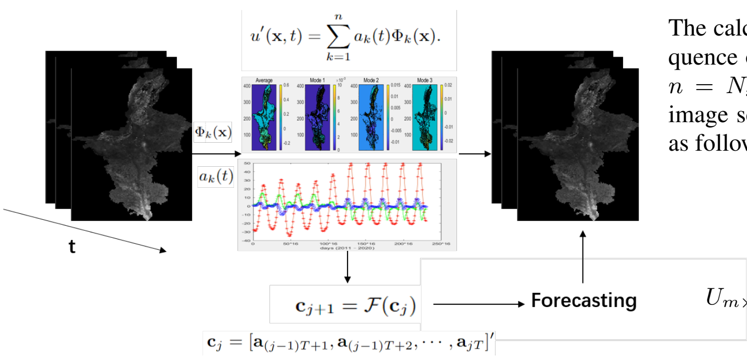

Figure 1. Conceptual workflow of latent space dynamics identification

2.2.2 POD: From Original Space to Latent Space The POD method effectively separates the temporal and spatial variation in flow fields by decomposing a time-varying flow field into a series of modes. Each mode consists of the product of a time-invariant spatial function (POD mode) and a purely time-dependent temporal function.The POD modes capture the dominant dynamic energy of flow field fluctuations, representing the principal spatiotemporal variations through a minimal set of modes. This approach provides an objective and quantitative characterization of both spatial structures and temporal evolution in flow fields (Back and Weigend, 1997).

Mathematically, the spatial POD modes can be obtained through eigen-analysis. Assuming that $u'(\mathbf{x}, t)$ is a fluctuating flow field, i.e., a time-averaged steady velocity field ($U - \bar{U}$) has been subtracted from the velocity vector, $\mathbf{x} = (x, y, z)$ is the position, and t is the time, POD is the decomposition of the random vector field $u'(\mathbf{x}, t)$ into a defined set of function spaces with random time coefficients $a_k(t)$, such that:

$$u'(\mathbf{x}, t) = \sum_{k=1}^{\infty} a_k(t)\Phi_k(\mathbf{x}) \tag{3}$$

The so-called ”P” of POD is to find the proper space such that $\sum_{k=1}^{n} a_k(t)\Phi_k(\mathbf{x})$ maximizes the dynamic energy through the first n spatial modes, and ”O” means that these modes are orthogonal, that is, in the appropriate function space:

$$\iiint_{\mathbf{x}} \Phi_{k_1}(\mathbf{x})\Phi_{k_2}(\mathbf{x})\, d\mathbf{x} = \begin{cases} 1, & k_1 = k_2 \\ 0, & k_1 \neq k_2 \end{cases} \tag{4}$$

The orthogonality is useful because it suggests that each time factor $a_k(t)$ depends only on the space mode $\Phi_k(\mathbf{x})$. This expression is obtained as:

$$a_k(t) = \iiint u'(x,t)\Phi_k(x)dx \tag{5}$$

When treating space and time as independent variables, POD maintains a fundamental symmetry between spatial and temporal dimensions. This decomposition can alternatively be interpreted as determining temporal modes through the regularization of random spatial coefficients, demonstrating the mathematical interchangeability of space and time in this framework. This symmetric formulation, known as the Snapshot POD method, was originally introduced by Sirovich (Sirovich, 1987).

The calculation process of POD is as follows: If the image sequence of a certain region NDVI is $U(\mathbf{x}, t)$, the image size is $n = N_x \times N_y$, and the time points are $m = N_t$, then the image sequence is subtracted from the mean to form a matrix as follows:

$$U_{m\times n} = \begin{pmatrix} u'(x_1, y_1, t_1) & \cdots & u'(x_N, y_N, t_1) \\ u'(x_1, y_1, t_2) & \cdots & u'(x_N, y_N, t_2) \\ \vdots & \ddots & \vdots \\ u'(x_1, y_1, t_m) & \cdots & u'(x_N, y_N, t_m) \end{pmatrix} \tag{6}$$

The covariance of the matrix U is denoted as C, that is $C =$

$\frac{1}{m-1}UU^T$. It is the matrix of $m \times m$. Calculate the eigenvectors of C, and get m eigenvectors $\lambda_1, \lambda_2, \cdots, \lambda_m$, generally from large to small order, and the corresponding m eigenvectors written as a $\Phi_k(\mathbf{x}), k = 1, 2, \cdots, m$. If the matrix U is projected on a matrix Φ (Φ_k is its column vector) as a matrix , then there is $A_{m\times m} = U_{m\times n}\Phi_{n\times m}$. Each column of A is a time coefficient Φ_k corresponding to $A_k = U\Phi_k$. The larger the characteristic root is, the more typical the spatial mode is and the greater the contribution to the total variance is. That is, the contribution of the first characteristic vector is:

$$\rho_k = \frac{\lambda_k}{\sum_{i=1}^{m} \lambda_i}, \quad k = 1, 2, \ldots, m \tag{7}$$

The contribution of the first characteristic vectors is $\sum_{i=1}^{p} \rho_i$. The cumulative variance contribution rate is the basis of retaining the order of spatial modes.

2.2.3 AM-HAR: Cycle-to-Cycle Dynamics We reconstruct a continuous-time dynamical model for these temporal coefficients using AM-HAR. This choice is motivated by the geometric relationship between the Earth and the Sun—specifically, Earth's rotation and its revolution with orbital inclination—which imposes a strong periodic background on land surface variations, primarily manifested as diurnal and annual cycles. However, the actual variation at any given location results from the superposition of such periodic signals with various non-periodic atmospheric and oceanic internal processes, as well as long-term trends.

AM-HAR is a natural choice for modeling the temporal coefficients, which typically exhibit strong seasonal and interannual rhythms. Its Amplitude-Modulated harmonic formulation captures the dominant frequency while accommodating asymmetries in seasonal waveforms (e.g., asymmetric growing and senescing phases in vegetation phenology), enabling it to represent both the strong periodicity and the variations between cycles. The resulting model thus balances physical interpretability with the flexibility to represent key features of land surface dynamics.

Considering that the MODIS data products used in this paper have an actual temporal resolution of 16 days, there are $T = 23$ time phases per year. This allows the remote sensing data with an annual cycle to be regarded as a periodic function with a period of $T = 23$, which is equivalent to applying a time transformation $t = t'/16$.

As periodicity is inherently present in remote sensing data, so the AM-HAR method here aims to discover interpretable dynamical models for the temporal coefficients between successive periods. Instead of imposing a rigid periodic structure, we treat the problem as learning a mapping from the current cycle to the next cycle. Let $\mathbf{c}_j \in \mathbb{R}^T$ denote the j-th cycle of the original data, and let $\mathbf{c}_j = [\mathbf{a}_{(j-1)T+1}, \mathbf{a}_{(j-1)T+2}, \cdots, \mathbf{a}_{jT}]'$. We learn a predictive model:

$$\mathbf{c}_{j+1} = \mathcal{F}(\mathbf{c}_j) + \boldsymbol{\varepsilon}_j \tag{8}$$

where $\mathcal{F}$ is a mapping to be learned from data representing the evolution relationship between different cycles. Training data pairs are constructed by using the current cycle to predict the next cycle,that is, to train model $\mathcal{F}$ such that:

$$\mathbf{c}_{\text{input}} = \mathbf{c}(:, 1 : n_{\text{cycles}} - 1), \quad \mathbf{c}_{\text{output}} = \mathbf{c}(:, 2 : n_{\text{cycles}}).$$

The process of training and computing $\mathcal{F}$ is as follows:

(1) Intra-period harmonic function construction

Given a periodic sequence with period length T, the data for cycle j, $\mathbf{c}_j \in \mathbb{R}^T$, is represented by harmonic analysis as:

$$c_j(t) = a_{0,j} + \sum_{k=1}^{K} \left[a_{k,j} \cos\left(\frac{2\pi kt}{T}\right) + b_{k,j} \sin\left(\frac{2\pi kt}{T}\right) \right] + \varepsilon_j(t) \tag{9}$$

where $t = 0, 1, \ldots, T-1$ is the intra-cycle position index,$a_{0,j}$ is the constant term, $a_{k,j}, b_{k,j}$ are the coefficients for the frequency $\omega_k = 2\pi k/T$,$\varepsilon_j(t)$ is the random error term.These coefficients vary with j, reflecting variations across periods.

Define the basis function matrix $\mathbf{\Psi} \in \mathbb{R}^{T\times(2K+1)}$:

$$\mathbf{\Psi} = \begin{bmatrix} 1 & \cos(\omega_0 t_0) & \sin(\omega_0 t_0) & \cdots & \cos(2\omega_K t_0) & \sin(2\omega_K t_0) \\ 1 & \cos(\omega_0 t_1) & \sin(\omega_0 t_1) & \cdots & \cos(2\omega_K t_1) & \sin(2\omega_K t_1) \\ \vdots & \vdots & \vdots & \cdots & \vdots & \vdots \\ 1 & \cos(\omega_0 t_{T-1}) & \sin(\omega_0 t_{T-1}) & \cdots & \cos(2\omega_K t_{T-1}) & \sin(2\omega_K t_{T-1}) \end{bmatrix} \tag{10}$$

The model can be expressed in matrix form as:

$$\mathbf{c}_j = \mathbf{\Psi}\boldsymbol{\beta}_j + \boldsymbol{\varepsilon}_j \tag{11}$$

where $\boldsymbol{\beta}_j = [a_{0,j}, a_{1,j}, b_{1,j}, \cdots, a_{K,j}, b_{K,j}]^T$ is the coefficient vector for cycle j.

$\boldsymbol{\beta}_j$ is estimated via Ridge estimation using the first N_{train} cycles with an L_2 regularization term added to the objective function:

$$||\mathbf{c}_j - \mathbf{\Psi}\hat{\boldsymbol{\beta}}_j||_2^2 + \lambda|\hat{\boldsymbol{\beta}}_j|_2^2 \tag{12}$$

The closed-form solution of $\boldsymbol{\beta}_j$ is:

$$\hat{\boldsymbol{\beta}}_j^{(\lambda)} = (\mathbf{\Psi}^T\mathbf{\Psi} + \lambda\mathbf{I})^{-1}\mathbf{\Psi}^T\mathbf{c}_j \tag{13}$$

where $\lambda \geq 0$ is the regularization parameter and $\mathbf{I} \in \mathbb{R}^{(2K+1)\times(2K+1)}$ is the identity matrix.

(2) Inter-period trend estimation

Based on the estimation of $\boldsymbol{\beta}_j$, a trend model for the coefficients is considered. Each coefficient $\beta_j^{(i)}$ $(i = 1, \ldots, 2K+1)$ is assumed to evolve linearly with cycle index j:

$$\beta_j^{(i)} = c_i + d_i \cdot j + \eta_j^{(i)} \tag{14}$$

where c_i is the intercept, d_i is the trend slope, and $\eta_t^{(i)}$ is the residual.

Trend Estimation using the first N_{train} cycles, the trend parameters are estimated via least squares as

$$\hat{\beta}_j^{(i)} = c_i + d_i \cdot j \tag{15}$$

The coefficients are predicted also used for extrapolation for future cycles $j > N_{\text{train}}$.

For a test cycle j, the predicted coefficient vector is:

$$\hat{\boldsymbol{\beta}}_j = [\hat{\beta}_j^{(1)}, \hat{\beta}_j^{(2)}, \ldots, \hat{\beta}_j^{(2K+1)}]^T \tag{16}$$

(3) Prediction and reconstruction

The predicted temporal cycle data for $j > N_{\text{train}}$ is reconstructed using the basis functions:

$$\hat{\mathbf{c}}_j = \boldsymbol{\Psi}\hat{\boldsymbol{\beta}}_j \tag{17}$$

For forecasting, we iterate the learned dynamical model starting from an initial observed cycle:

$$\hat{\mathbf{c}}_{j+1} = \mathcal{F}(\hat{\mathbf{c}}_j), \quad \hat{\mathbf{c}}_1 = \mathbf{c}_1 \tag{18}$$

where $\hat{\mathbf{c}}_j$ denotes the predicted latent coefficients. Remember that $\mathbf{c}_j = [\mathbf{a}_{(j-1)T+1}, \mathbf{a}_{(j-1)T+2}, \cdots, \mathbf{a}_{jT}]'$, the predicted high-dimensional fields are then reconstructed using the precomputed POD basis:

$$\hat{\mathbf{u}}_t = \boldsymbol{\Phi}\hat{\mathbf{a}}_t \tag{19}$$

Sofar the POD-AM-HAR method provides a simple regression framework for discovering a generally nonlinear model for the evolution dynamics of the high-dimensional model in a low-dimensional subspace.

3. Results and Discussions

3.1 Dynamic analysis of ten-year data

Fig. 2 presents the spatial distribution of the mean MODIS NDVI values (2011-2020) across Ningxia's 230 temporal phases and the eigenvectors corresponding to the first three POD modes. Table 3 displays the eigenvalues for the first five POD modes, revealing that these modes collectively explain 97.18% of the total variance, with the first mode alone accounting for 87.4% and the first three modes contributing 95.24% of the variance. The complete eigenvalue spectrum (230 modes) is shown in Fig. 4. The temporal coefficient curves for the first three eigenvectors (Fig. 5) exhibit clear periodicity. The first temporal coefficient demonstrates a distinct greening trend in Ningxia's vegetation over the study period:

- A significant increase from 2011 to 2015
- Relative stability from 2016 to 2020
- Consistent annual phenological patterns, peaking in July before browning - a pattern that aligns with Ningxia's climatic characteristics

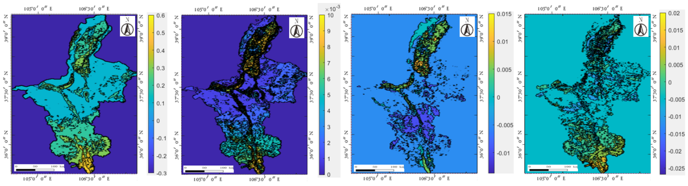

Figure 2. Mean spatial distribution and first three modes of NDVI data of ten years in Ningxia by POD(filled with Contours)

Mode	Eigenvalue	Variance Contribution Rate(%)	Cumulative Variance Contribution Rate(%)
1	568.4896	0.8740	0.8740
2	40.3732	0.0621	0.9361
3	10.5927	0.0163	0.9524
4	9.8712	0.0152	0.9676
5	2.7082	0.0042	0.9718

Figure 3. The first five eigenvalues, the contribution rate and the total contribution rate of the POD

The second temporal coefficient shows amplitude variations between two distinct periods:

- Higher amplitudes during 2011-2016, suggesting active urban/industrial development
- Reduced amplitudes in 2017-2020, indicating stabilization

The third temporal coefficient reveals differences between 2011-2015 and 2016-2020, reflecting vegetation dynamics associated with Loess Plateau greening in sub-humid regions. These variations correspond to different developmental stages in the region. Through POD decomposition, we established that the system's evolution in the reduced-dimensional subspace (comprising the first three spatial modes) is primarily governed by these three temporal coefficients.

3.2 Predictive performance analysis

Based on the preceding analysis, land surface dynamics underwent a change around the year 2015. Therefore, we designed three experimental groups as follows:

Model_5 built using data from 2011 to 2015 to predict 2016–2020;

Model_6 built using data from 2011 to 2016 to predict 2017–2020;

Model_7 built using data from 2011 to 2017 to predict 2018–2020.

After POD decomposition, dynamic models need to be constructed for the coefficients $a_1(t)$, $a_2(t)$, and $a_3(t)$, which are

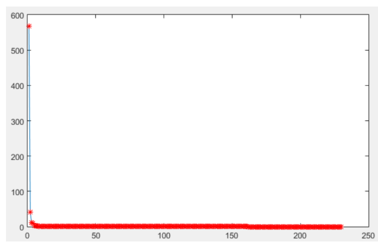

Figure 4. The 230 eigenvalues of POD

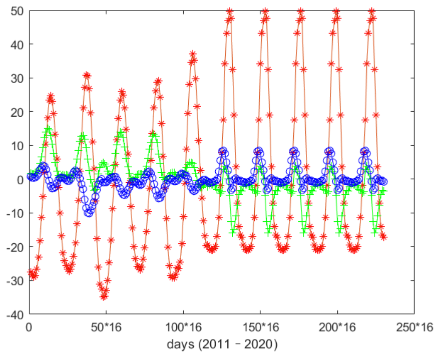

Figure 5. The time coefficients of the first three eigenvectors of NDVI in Ningxia.

shown in Fig. 5 with different colors. Using the AM-HAR algorithm, we construct Model_5, Model_6,and Model_7, respectively. Figs. 6 through 8 present the time coefficients alongside their corresponding predictions from the dynamic models, where the black lines denote the original coefficient curves, and the red, green, and blue lines represent the predicted values. From these figures, the following observations can be made:

- The training data contain no information about variations beyond the training period, resulting in lower predictive capability for Model_5 compared to Model_6 and Model_7;
- The predictive performance of the model also exhibits strong dependence on the last cycle within the training data;
- The linear trend assumption appears to restrict the model's ability to capture nonlinear inter-cycle variations.

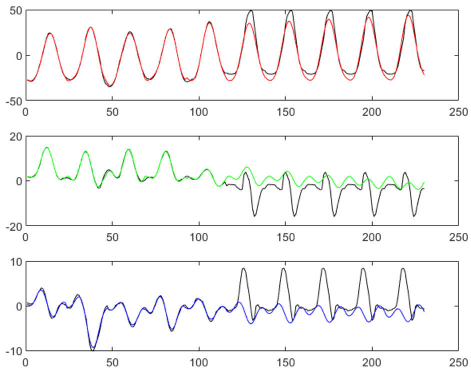

Figure 6. The time coefficients of Model_5 and their predictions by dynamic model

Using the time coefficients predicted by different dynamic models, combined with the spatial modes obtained from POD, the NDVI images are reconstructed according to Equation (19). Different dynamic models yield different prediction accuracies, which in turn result in varying reconstruction accuracies. Figures 9 to 11 show the error curves of the reconstructed image sequences corresponding to Model_5, Model_6, and Model_7, respectively. The error of every NDVI image is calculated by

$$\epsilon(t) = \|\mathbf{u(t)} - \hat{\mathbf{u}}(\mathbf{t})\|_2^2/(N_x * N_y)$$

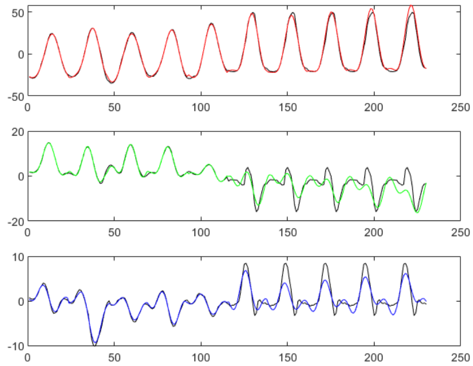

Figure 7. The time coefficients Model_6 and their predictions by dynamic model

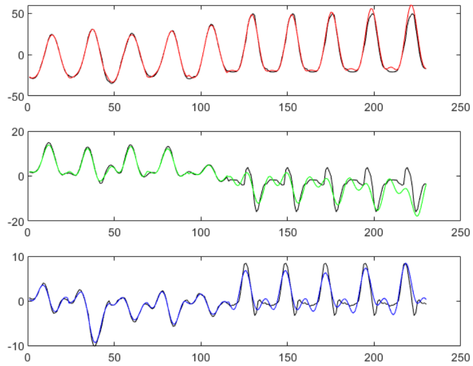

Figure 8. The time coefficients Model_7 and their predictions by dynamic model

Figures 9 to 11 reveal that

- Model_5 does not predict future changes well.Compared to Model_5,Model_6 and Model_7 can better capture the 10-year evolution patterns in the Ningxia region, as the evolution from 2016 to 2020 is relatively consistent with the training period.
- Due to the excellent fitting and approximation capabilities of harmonic functions for periodic signals, the dynamic evolution of Model_5 to Model_7 within the training period closely matches the actual evolution, resulting in relatively low reconstruction errors for the images during this period.

Fig. 12 shows the reconstructed NDVI imagesusing the prediction results of Model-6 (trained with the first 138 frames), specifically for frames 197 and 200. The upper panels show the original images, while the lower panels show the images reconstructed based on POD-AM-HAR, the reconstruction errors are 3.5746e-04 and 3.5768e-04, and the corresponding error-to-mean ratios of the images are 0.79% and 0.76%, respectively.

4. Conclusions

In this study, the proposed POD-AM-HAR framework provides an effective approach for constructing dynamic models that

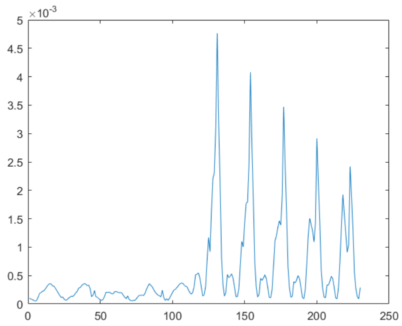

Figure 9. The error curve of $\epsilon(t)$ by Model_5

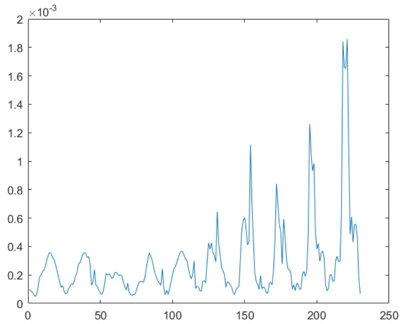

Figure 10. The error curve of $\epsilon(t)$ by Model_6

characterize typically nonlinear high-dimensional evolution dynamics within a latent subspace. The method shifts the modeling mode from point-wise dynamics to cycle-based dynamics, successfully capturing spatiotemporal patterns while maintaining periodicity and predictive capability over extended temporal scales, and adapting to inter-cycle variations. The results exhibit strong spatiotemporal consistency.

The core of the POD-AM-HAR framework is to construct dynamic models in the latent space based on temporal evolution characteristics. Considering the strong periodic nature of remote sensing data, we propose a cycle-based amplitude-modulated harmonic analysis method, combined with linear trend extrapolation and Ridge regularization, for forecasting periodic land surface dynamics. The model decomposes each annual cycle into a constant term and dominant frequency components, capturing both the primary seasonal oscillation and the waveform asymmetry inherent in vegetation phenology, while preserving physically meaningful representations. The temporal evolution of the coefficients is modeled using linear trends, reflecting the gradual interannual changes in vegetation productivity, phenological timing, and seasonal amplitude.

Experimental results on ten years of MODIS NDVI data from the Ningxia region, China, demonstrate that the proposed method achieves reasonable predictive performance under different configurations. The method exhibits several key advantages: (1) strong physical interpretability, as each coefficient corresponds to a meaningful ecological quantity; (2) high computational efficiency due to closed-form solutions; (3) low data requirements, making it suitable for applications with limited historical observations; and (4) stable extrapolation capability via linear trend modeling.

However, the method also has inherent limitations. The linear trend assumption restricts its ability to model nonlinear interannual variations or abrupt changes such as disturbances or regime shifts. Additionally, the fixed periodic assumption may not accommodate phenological shifts caused by climate variability. Future work could extend this framework by incorporating adaptive harmonic selection, nonlinear trend modeling, or integrating external covariates such as climate variables to improve predictive accuracy under non-stationary conditions.

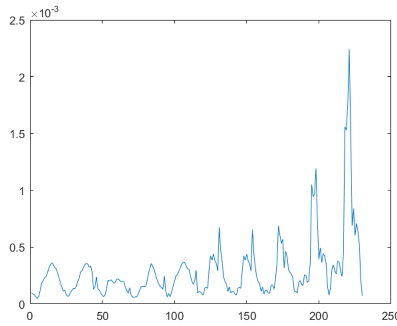

Figure 11. The error curve of $\epsilon(t)$ by Model_7

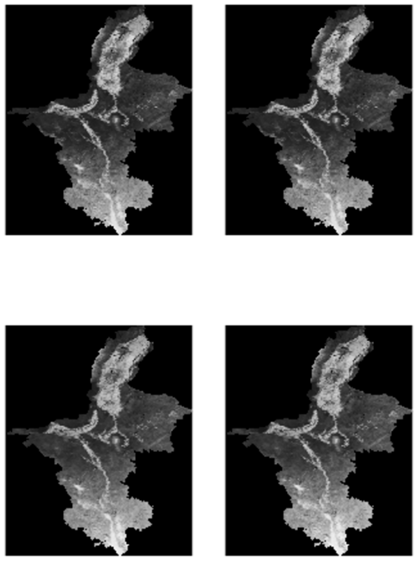

Figure 12. NDVI images at phases 197 and 200 predicted by the 6-cycle model. Upper: original; lower: predicted.

References

Back, A. D., Weigend, A. S., 1997. A First Application of Independent Component Analysis to Extracting Structure from Stock Returns. *Econometrics: Applied Econometrics Modeling eJournal*.

Gao, J., 2024. Intrinsic simplicity of complex systems. *Nature Physics*, 20, 184–185. doi.org/10.1038/s41567-023-02268-0.

Sirovich, L., 1987. Turbulence and the dynamics of coherent structures, part I:coherent structures. *Q. Appl.Math.*, XLV(6), 561-572.